Title

Bone marrow uptake of indolent non-Hodgkin lymphoma on PET/CT with histopathological correlation.

Abstract

Objective

To evaluate the diagnostic accuracy of PET/CT in detecting marrow infiltration in indolent non-Hodgkin lymphoma(NHL) with histopathological correlation.

Methods

All treatment-naive newly diagnosed indolent NHL with staging PET/CT were retrospectively evaluated for marrow infiltration and categorized based on PET/CT uptake pattern: normal (PET/CT negative, -ve), focal/diffuse (PET/CT positive, +ve). Bone marrow biopsy (BMB)was taken as the standard except in focal PET/CT uptake, which was confirmed to be positive or negative by serial PET/CT. BMB pattern was assessed as diffuse and non-diffuse, and degree of lymphoid infiltration documented.

Results

Forty-six patients (mean age 59±15 years) were evaluated. In the PET/CT +ve group of 22 cases (diffuse=15, focal=7), BMB was positive in 21 cases. In 80% of diffuse PET/CT uptake cases, a diffuse BMB infiltrative pattern was observed. However, in cases with focal PET/CT uptake, no predominant histological pattern was observed. No correlation was found between semi-quantitative uptake and degree of lymphoid infiltration on BMB (r=0.2, p=0.434). In the PET/CT –ve group of 24 cases, 20 cases were BMB negative and 4 cases were positive. The overall diagnostic accuracy of PET/CT in determining marrow infiltration was 89% (sensitivity 84%, specificity 95%, positive predictive value 95% and negative predictive value 83%).

Conclusion

PET/CT showed high specificity and positive predictive value with moderate accuracy in detecting marrow disease in indolent NHL. The metabolic uptake lacked significant correlation with the degree of lymphoid infiltration but a potential relationship may exist between pattern of metabolic uptake and BMB infiltrative pattern.

Keywords

Indolent lymphoma; bone marrow; marrow biopsy; PET/CT; SUV

Introduction

Bone marrow (BM) infiltration in lymphoma upstages the disease based on the Ann Arbor staging system. In prognostic models for both aggressive and indolent lymphomas, BM infiltration is a significant negative predictor of disease outcome [1, 2]. Hence, accurate assessment of BM infiltration forms an important part of lymphoma staging, and is conventionally based on BM aspirate (BMA) and trephine biopsy (BMB). However, BM infiltration can be heterogeneous and focal, so that sampling error might compromise the accuracy of BMA/BMB. Furthermore, BMA/BMB is an invasive procedure with potential complications [3, 4].

In Hodgkin lymphoma (HL), recent evidence suggests that fused position emission tomography and computed tomography (PET/CT) could replace BMB [5]; whilst in aggressive non-Hodgkin lymphoma (NHL) of diffuse large B-cell subtype, a recent meta-analysis suggests that a positive PET/CT obviates the need of BMB [6]. However, there is currently insufficient evidence that the same can be applied in indolent NHL, largely due to the lower FDG avidity of indolent NHL, resulting in reduced sensitivity of PET/CT [7-9]. Furthermore, indolent NHL is a group of heterogeneous diseases with variable patterns of marrow infiltration on BMB, which may further confound the marrow activity on PET/CT [10, 11].

PET/CT is increasingly used in the evaluation of indolent NHL, especially at detecting disease transformation, which may lead to treatment modification and disease prognostication [12-16].Several studies demonstrated moderate to high specificity (86-96%) of positive PET/CT marrow uptake in determining disease infiltration in different subtypes of indolent NHL, but these studies were limited by inclusion of relapsed patients whose marrow uptake might have been affected by previous intensive chemotherapy. There was also a lack of follow-up imaging to verify marrow uptake that was not concordant with BMB [17-19]. Finally, the correlation between marrow FDG uptake patterns and the histological evaluation with BMB remains unexplored. Herein, we aimed at evaluating the diagnostic accuracy of PET/CT in detecting bone marrow infiltration in indolent NHL with histopathological correlation.

Methods

Patients

All consecutive staging PET/CT examinations with histological confirmed treatment-naïve newly diagnosed indolent NHL from April 2007-March 2014 in one single centre were retrospectively reviewed. Patients with a history of previous radiation therapy, concurrent infection or recent granulocyte colony-stimulating factor (G-CSF) injections that might affect marrow uptake were excluded. The diagnosis of lymphoma was based on the 2008 WHO classification system [20] and grouped as indolent NHL based on the subtypes and clinical prognoses [21]. The local institutional research and ethics review board approved this retrospective study and waived the need for informed consent.

Bone marrow assessment

Bilateral BMA and BMB were performed in all patients. Morphological assessment, flow cytometric analysis, evaluation of percentage of lymphoid infiltration and immunohistochemical studies were performed, according to the 2008 WHO classification system [20]. For cases diagnosed prior to 2008, patients were retrospectively reviewed and reclassified. The pattern of marrow infiltration on trephine biopsy was evaluated as previously described [11, 22, 23]. These were classified as non-diffuse(focal non-paratrabecular, focal paratrabecular and intrasinusoidal) or diffuse (diffuse interstitial and diffuse solid).

PET/CT

All PET/CT examinations were acquired on a dedicated PET/CT scanner (Discovery VCT, 64-multislice CT, GE Healthcare Bio-Sciences Corp.). Patients were requested to fast 6 hours before PET/CT and serum glucose should not exceed 180mg/dl prior to injection of 10mCi (370MBq) 18F-fluoro-deoxyglucose (FDG). Acquisition of images was performed 60 minutes following FDG injection. For patients who had no prior diagnostic CT, the CT was performed with intravenous contrast medium using the following imaging parameters: field of view; 50 cm; pixel size, 3.91 mm; 120 kVp; 200–400 mA; 0.5 s/CT rotation, pitch 0.984:1; 2.5 mm intervals; 1.5 mL/kg intravenous contrast medium injected at a rate of 2.0mL/second. Otherwise, low-dose CT was performed for attenuation correction with 80–200 mA and keeping other imaging parameters identical to the diagnostic CT acquisition. Each scan covered

from the skull base to both the upper thighs. PET images were reconstructed using an ordered-subset expectation maximization iterative algorithm (14 subsets and two iterations), and CT was used for attenuation correction of the PET emission data. PET was analyzed on a dedicated PET/CT ADW4.3 workstation (GE Healthcare, Milwaukee, WI), with a consensus reached by two radiologists (EL and PL, 4 years and 7 years PET/CT experience respectively), who were blinded to the BMB results at the time of review. PET data presented in maximum intensity projection (MIP) was qualitatively evaluated and categorized into 3 patterns: (a)*normal* when BM metabolic uptake is lower than background liver metabolic uptake (PET/CT negative, –ve), (b) *diffuse* in the presence of generalized homogeneous marrow uptake equal or increased compared to liver (PET/CT positive, +ve), and (c) *focal* in the presence of localized region of increased FDG activity with or without corresponding CT osseous destruction or density change (PET/CT positive, +ve). CT features suggestive of benign or malignant osseous tumours were evaluated; these included systematically assessing the zone of transition, presence or absence of periosteal reaction and cortical destruction, and the underlying matrix and marrow density. Focal marrow uptake that corresponded to benign osseous lesion was excluded. The region of interest (ROI) was defined in areas with focal marrow uptake to quantify the pixel with the highest FDG uptake, normalized against lean body mass, giving the maximum standardized uptake value, denoted here as SUV_{BM}. In the presence of multifocal uptake foci, the site with the highest uptake would be selected for quantification. In normal and diffuse PET/CT marrow uptake pattern, a standard sized ROI (1 cm^3) was placed in 4^{th} lumbar vertebra body to quantify the SUV_{L4}. The background liver uptake was taken as internal reference given its low intra-patient variability [24, 25]. The maximum FDG uptake in the liver was derived from placing a1 cm^3 ROI in the centre of the right hepatic lobe (SUV_{liver}). Metabolic ratio was defined as SUV_{L4}/SUV_{liver}.

Standard of reference

BMB was taken as standard of reference in PET/CT with normal or diffuse uptake pattern. In patient with focal uptake on PET/CT away from BMB sites and was discordant with BMB results, verification of focal uptake was based on serial PET/CT. True positive uptake was assumed when the lesion responded concordantly with the overall disease status following treatment, as evaluated with the Cheson's criteria (complete response, partial response, stable disease or progressive disease)

[26]; whereas marrow uptake discordant with the overall disease status on follow-up was taken as false positive osseous focus.

Statistical analysis

Clinical data and metabolic parameter were presented as mean and standard deviation (mean ±s.d.) with descriptive statistics. The diagnostic accuracy was evaluated by sensitivity, specificity, positive predictive value (PPV) and negative predictive value (NPV). Mann-Whitney U test evaluated the difference in the metabolic ratio between PET/CT –ve and diffuse PET/CT +ve groups. Non-parametric Spearman's rank correlation assessed the relationship between SUV and degree of lymphoid infiltration on BMA. All statistical analysis was performed using SPSS for Windows (version 20; SPSS Inc., Chicago, Illinois, USA).

Results

Clinical demographics

The study population comprised 46patients (men:23; women:23) at 59±15 years old with indolent NHL (follicular lymphoma, *n*=11;lymphoplasmacytic lymphoma, *n*=12; mucosa-associated lymphoid tissue lymphoma, *n*=12; nodal marginal zone B-cell lymphoma, *n*=4; small lymphocytic lymphoma, *n*=1; low-grade B cell unclassifiable, *n*=6). None of the patients had histological evidence of large cell transformation, which would otherwise be treated as aggressive lymphoma. The interval between PET/CT and BMB was 4±9 days.

PET/CT +ve with diffuse uptake pattern (*n*=15)

All but one (14/15, 93%) cases had PET/CT findings concurring with BMB findings (SUV_{L4}/ SUV_{liver} 1.7±1.6; Fig. 1). One patient was PET/CT +ve but BMB was negative, resulting in one false positive. Twelve out of the 15 (80%) PET/CT +ve patients had diffuse marrow infiltration pattern and 2 (13%) patients had focal paratrabecular non-diffuse marrow infiltration pattern on BMB. Of note, 5 patients with diffuse marrow infiltration pattern also had concurrent non-diffuse pattern in sub-regions of the trephine samples. The lymphoid cells involvement ranged from 5-90% (60 ± 27%, *n*=13).

PET/CT +ve with focal uptake pattern (*n*=7)

There was high concordance between focal uptake pattern on PET/CT with BMB (6/7, 86%; Fig. 2). No predominant marrow infiltration pattern was identified with even distribution of diffuse (*n*=3) and non-diffuse (*n*=3) marrow patterns on BMB. The lymphoid cells involvement ranged from 38-69% (51 ± 16%, *n*=3). Only one patient had discordant finding with a uninvolved BMB, due to focal uptake in the right femur, corresponding to focal marrow hyperdensity on CT. Interim PET/CT 3 months later after 3 cycles of R-CHOP chemotherapy regimen demonstrated resolution of the right femoral activity, together with complete response in the other non-BM deposits (Fig. 3). Therefore, this case probably represented real marrow infiltration that was missed on BMB. The mean focal marrow uptake was SUV_{BM} 3.8±1.2.

PET/CT –ve (*n*=24)

Twenty patients with normal marrow uptake (SUV_{L4}/ SUV_{liver} 0.8±0.2) concurred with negative BMB. The marrow metabolic ratio was significantly lower than PET/CT +ve group ($p<0.001$). There were 4 false negative (SUV_{L4}/ SUV_{liver} 0.7±0.1) cases from two follicular lymphoma, one low-grade B cell lymphoma and one small lymphocytic lymphoma. Two patients had concurrent diffuse and non-diffuse infiltration patterns on BMB whilst the other two patients had diffuse interstitial marrow infiltration pattern only. Three of these patients had moderate lymphoid cells involvement on BMA, ranging from 50-86% (72± 19%).

Relationship between SUV and degree of lymphoid infiltration

In our cohort, only 19 patients had positive BMA allowing for the evaluation of lymphoid infiltration degree. No statistical significant trend was observed between the marrow metabolic ratio and the degree of lymphoid infiltration (r=0.2, p=0.434).

Diagnostic characteristics

The overall accuracy of PET/CT in detecting BMI was 89% (41/46) with sensitivity of 84% (21/25), specificity of 95% (20/21), PPV 95% (21/22) and NPV 83% (20/24). In comparison, BMB has accuracy of 98% (45/46), sensitivity of 96% (24/25), specificity of 100% (21/21), PPV 100% (24/24) and NPV95% (21/22) (Table 1).

Discussion

The role of PET/CT in assessing marrow infiltration in indolent NHL is less well evaluated compared with aggressive NHL [6]. Our study showed that PET/CT was useful in diagnosing marrow infiltration given the high PPV and specificity, but was unable to replace BMB in view of the moderate sensitivity and NPV of PET/CT. Our study provided histopathological correlation in explaining the detectable FDG marrow avidity in indolent NHL, in that diffuse PET/CT uptake was associated with diffuse BMB pattern in 80% of the cases. However, the lack of significant correlation between metabolic ratio and degree of lymphoid infiltration suggested that the PET/CT uptake was not only dependent on the amount of lymphoid cells, but also the density of infiltration in terms of marrow infiltrative pattern on BMB.

Indolent NHL is associated with higher incidence of marrow infiltration compared with aggressive lymphoma [27]. The marrow infiltration pattern is known to be related to histological subtypes. In particular, the paratrabecular pattern is more commonly associated with follicular lymphoma and less commonly with marginal zone B-cell lymphoma [11]. In our cohort, we observed an association between diffuse PET/CT marrow uptake and diffuse infiltration pattern on BMB. This finding would require further investigation in larger cohort to ascertain its significance. This is different in HL and aggressive NHL, where diffuse marrow uptake pattern could be attributed to inflammation and cytokine release [21, 28, 29]. This is especially true in HL where the microenvironment is dominated by extensive inflammatory cellular infiltrates with small fraction of tumour cells [30].

The advantage of PET/CT in detecting focal marrow disease was supported by our findings. PET/CT was more sensitive than BMB in one patient, where the iliac biopsy sites were non-FDG avid, likely illustrating the issue of sampling error with BMB [3, 19]. Though no targeted biopsy was performed, we took care in verifying the discordant finding through analyzing the CT feature and the metabolic changes after chemotherapy [28]. Focal marrow uptake on PET/CT could potentially obviate BMB or even targeted re-biopsy of the sites with increased FDG avidity in indolent NHL, different to that suggested in aggressive NHL and HL that requiring re-examination of the FDG positive marrow sites [31].

Concordant with others, a negative PET/CT could not replace BMB, because of the high false negative rate of 17% (4/24) and only a moderate sensitivity of 84% (21/25) [7-9, 32]. We propose that the relatively lower and heterogeneous FDG avidity in indolent NHL, and low density in marrow involvement could explain these discordant findings between BMB and PET/CT [8, 10].
The semi-quantitative analysis of the marrow uptake showed that significantly higher metabolic ratio was observed in the PET/CT +ve compared to PET/CT –ve groups, and the present findings are in line with two recent studies that showed added values of semi-quantitative evaluation over visual PET/CT analysis in marrow assessment [17, 19].

Our study was limited by the small number of patients with various histological subtypes of indolent-NHL that introduced study heterogeneity. However, we only included cases evaluated before treatment and excluded cases that could have metabolic marrow changes induced by non-lymphomatous factors, thus making the marrow evaluation more objective. None of the focal PET/CT marrow +ve lesions were biopsied to confirm histological infiltration, and the follow-up PET/CT was used as surrogate clinical marker in one discordant case. This could potentially introduce bias as inflammatory or benign bone lesion could be FDG avid. However, the CT feature and responsiveness following chemotherapy were supportive of lymphomatous involvement and consensus was reached through careful multidisciplinary discussion. Other marrow foci with focal uptake were concordant with BMB findings, so that it could be considered clinically unnecessary to re-biopsy these areas with focal activities given the lack of impact on clinical management.

Conclusion

PET/CT has high specificity and PPV in detecting marrow disease infiltration in indolent NHL, but is not sensitive enough to replace BMB. The metabolic uptake lacked significant correlation with degree of lymphoid infiltration but a potential relationship may exist between pattern of metabolic uptake and BMB infiltrative pattern. Patients with definite PET/CT marrow +ve findings might not necessarily need a BMB, whereas patients with PET/CT -ve marrow findings will benefit from histological confirmation.

Conflict of interest

There was no conflict of interest.

References

1. A predictive model for aggressive non-Hodgkin's lymphoma. The International Non-Hodgkin's Lymphoma Prognostic Factors Project. *N Engl J Med* 1993;**329**:987-994.
2. Federico M, Bellei M, Marcheselli L, Luminari S, Lopez-Guillermo A, Vitolo U, *et al.* Follicular lymphoma international prognostic index 2: a new prognostic index for follicular lymphoma developed by the international follicular lymphoma prognostic factor project. *J Clin Oncol* 2009;**27**:4555-4562.
3. Menon NC, Buchanan JG. Bilateral trephine bone marrow biopsies in Hodgkin's and non-Hodgkin's lymphoma. *Pathology* 1979;**11**:53-57.
4. Bain BJ. Morbidity associated with bone marrow aspiration and trephine biopsy - a review of UK data for 2004. *Haematologica* 2006;**91**:1293-1294.
5. Adams HJ, Kwee TC, de Keizer B, Fijnheer R, de Klerk JM, Littooij AS, *et al.* Systematic review and meta-analysis on the diagnostic performance of FDG-PET/CT in detecting bone marrow involvement in newly diagnosed Hodgkin lymphoma: is bone marrow biopsy still necessary? *Ann Oncol* 2014; **25**: 921-927.
6. Adams HJ, Kwee TC, de Keizer B, Fijnheer R, de Klerk JM, Nievelstein RA. FDG PET/CT for the detection of bone marrow involvement in diffuse large B-cell lymphoma: systematic review and meta-analysis. *Eur J Nucl Med Mol Imaging* 2014; **41**: 565-574.
7. Muslimani AA, Farag HL, Francis S, Spiro TP, Chaudhry AA, Chan VC, *et al.* The utility of 18-F-fluorodeoxyglucose positron emission tomography in evaluation of bone marrow involvement by non-Hodgkin lymphoma. *Am J Clin Oncol* 2008;**31**:409-412.
8. Elstrom R, Guan L, Baker G, Nakhoda K, Vergilio JA, Zhuang H, *et al.* Utility of FDG-PET scanning in lymphoma by WHO classification. *Blood* 2003;**101**:3875-3876.
9. Jerusalem G, Beguin Y, Najjar F, Hustinx R, Fassotte MF, Rigo P, *et al.* Positron emission tomography (PET) with 18F-fluorodeoxyglucose (18F-

FDG) for the staging of low-grade non-Hodgkin's lymphoma (NHL). *Ann Oncol* 2001;**12**:825-830.

10. Moog F, Bangerter M, Kotzerke J, Guhlmann A, Frickhofen N, Reske SN. 18-F-fluorodeoxyglucose-positron emission tomography as a new approach to detect lymphomatous bone marrow. *J Clin Oncol* 1998;**16**:603-609.
11. Torlakovic E, Torlakovic G, Brunning RD. Follicular pattern of bone marrow involvement by follicular lymphoma. *Am J Clin Pathol* 2002;**118**:780-786.
12. Barrington SF, Mikhaeel NG. Imaging follicular lymphoma using positron emission tomography with [(18)F]fluorodeoxyglucose: to what purpose? *J Clin Oncol* 2012;**30**:4285-4287.
13. Federico M, Luminari S, Dondi A, Tucci A, Vitolo U, Rigacci L, *et al.* R-CVP versus R-CHOP versus R-FM for the initial treatment of patients with advanced-stage follicular lymphoma: results of the FOLL05 trial conducted by the Fondazione Italiana Linfomi. *J Clin Oncol* 2013;**31**:1506-1513.
14. Le Dortz L, De Guibert S, Bayat S, Devillers A, Houot R, Rolland Y, *et al.* Diagnostic and prognostic impact of 18F-FDG PET/CT in follicular lymphoma. *Eur J Nucl Med Mol Imaging* 2010;**37**:2307-2314.
15. Wohrer S, Jaeger U, Kletter K, Becherer A, Hauswirth A, Turetschek K, *et al.* 18F-fluoro-deoxy-glucose positron emission tomography (18F-FDG-PET) visualizes follicular lymphoma irrespective of grading. *Ann Oncol* 2006;**17**:780-784.
16. Leleu X, Xie W, Bagshaw M, Banwait R, Leduc R, Roper N, *et al.* The role of serum immunoglobulin free light chain in response and progression in waldenstrom macroglobulinemia. *Clin Cancer Res* 2011;**17**:3013-3018.
17. Adams HJ, Kwee TC, Fijnheer R, Dubois SV, Blase PE, Nievelstein RA, *et al.* Utility of quantitative FDG-PET/CT for the detection of bone marrow involvement in follicular lymphoma: a histopathological correlation study. *Skeletal Radiol* 2014;**43**:1231-1236.
18. Banwait R, O'Regan K, Campigotto F, Harris B, Yarar D, Bagshaw M, *et al.* The role of 18F-FDG PET/CT imaging in Waldenstrom macroglobulinemia. *Am J Hematol* 2011;**86**:567-572.
19. El-Najjar I, Montoto S, McDowell A, Matthews J, Gribben J, Szyszko TA. The value of semiquantitative analysis in identifying diffuse bone marrow involvement in follicular lymphoma. *Nucl Med Commun* 2014;**35**:311-315.

20. Campo E, Swerdlow SH, Harris NL, Pileri S, Stein H, Jaffe ES. The 2008 WHO classification of lymphoid neoplasms and beyond: evolving concepts and practical applications. *Blood* 2011;**117**:5019-5032.
21. Carr R, Barrington SF, Madan B, O'Doherty MJ, Saunders CA, van der Walt J, *et al.* Detection of lymphoma in bone marrow by whole-body positron emission tomography. *Blood* 1998;**91**:3340-3346.
22. Foucar K, McKenna RW, Frizzera G, Brunning RD. Bone marrow and blood involvement by lymphoma in relationship to the Lukes--Collins classification. *Cancer* 1982;**49**:888-897.
23. Jones SE, Rosenberg SA, Kaplan HS. Non-Hodgkin's lymphomas. I. Bone marrow involvement. *Cancer* 1972;**29**:954-960.
24. Boktor RR, Walker G, Stacey R, Gledhill S, Pitman AG. Reference range for intrapatient variability in blood-pool and liver SUV for 18F-FDG PET. *J Nucl Med* 2013;**54**:677-682.
25. Paquet N, Albert A, Foidart J, Hustinx R. Within-patient variability of (18)F-FDG: standardized uptake values in normal tissues. *J Nucl Med* 2004;**45**:784-788.
26. Cheson BD, Pfistner B, Juweid ME, Gascoyne RD, Specht L, Horning SJ, *et al.* Revised response criteria for malignant lymphoma. *J Clin Oncol* 2007;**25**:579-586.
27. Mittal BR, Manohar K, Malhotra P, Das R, Kashyap R, Bhattacharya A, *et al.* Can fluorodeoxyglucose positron emission tomography/computed tomography avoid negative iliac crest biopsies in evaluation of marrow involvement by lymphoma at time of initial staging? *Leuk Lymphoma* 2011;**52**:2111-2116.
28. Moulin-Romsee G, Hindie E, Cuenca X, Brice P, Decaudin D, Benamor M, *et al.* (18)F-FDG PET/CT bone/bone marrow findings in Hodgkin's lymphoma may circumvent the use of bone marrow trephine biopsy at diagnosis staging. *Eur J Nucl Med Mol Imaging* 2010;**37**:1095-1105.
29. Muzahir S, Mian M, Munir I, Nawaz MK, Faruqui ZS, Mufti KA, *et al.* Clinical utility of (1)(8)F FDG-PET/CT in the detection of bone marrow disease in Hodgkin's lymphoma. *Br J Radiol* 2012;**85**:e490-496.
30. Kuppers R. The biology of Hodgkin's lymphoma. *Nat Rev Cancer* 2009;**9**:15-27.

31. Pakos EE, Fotopoulos AD, Ioannidis JP. 18F-FDG PET for evaluation of bone marrow infiltration in staging of lymphoma: a meta-analysis. *J Nucl Med* 2005;**46**:958-963.
32. Ngeow JY, Quek RH, Ng DC, Hee SW, Tao M, Lim LC, *et al.* High SUV uptake on FDG-PET/CT predicts for an aggressive B-cell lymphoma in a prospective study of primary FDG-PET/CT staging in lymphoma. *Ann Oncol* 2009;**20**:1543-1547.

Legends

Table 1. Comparison of BM assessment based on BMB and PET/CT. NHL: non-Hodgkin lymphoma; BMB: bone marrow biopsy; PET/CT: fused positron emission tomography and computed tomography; *n*: number; +ve: positive; -ve; negative; TP: true positive; TN: true negative; FP: false positive; FN: false negative.

Fig.1. PET/CT of patient with low-grade B cell lymphoma showing diffuse PET/CT uptake in the marrow that was confirmed to be involved by BMB.
(a) The MIP of PET/CT shows diffuse marrow uptake, visually more than the liver background activity (metabolic ratio, SUV_{L4}/SUV_{liver} 1.5).
(b) Sagittal CT image shows no corresponding abnormality in the axial skeleton.
MIP: maximum intensity projection; PET/CT: fused positron emission tomography and computed tomography; BMB: bone marrow biopsy.

Fig.2. PET/CT of patient with follicular lymphoma showing multifocal osseous uptake on background of diffuse uptake; corresponding to positive iliac BMB.
(a) Coronal PET image shows diffuse marrow uptake, visually more than the liver background activity (metabolic ratio, SUV_{L4}/SUV_{liver} 1.2).
(b) Sagittal fused PET/CT image shows diffuse marrow uptake in the axial skeleton, in addition to conglomerate markedly hypermetabolic retroperitoneal nodal masses (up to SUVmax 8.9).
(c) Axial fused PET/CT image shows focal marrow uptake at the right greater trochanter (white arrow, SUV_{BM} 2.9).
(d) Corresponding axial CT shows focal sclerosis at the right greater trochanter (white arrow).

PET/CT: fused positron emission tomography and computed tomography; BMB: bone marrow biopsy; SUVmax: maximum standardized uptake value; SUV_{BM}: maximum standardized uptake value of focal uptake.

Fig. 3. PET/CT of patient with focal PET/CT uptake but negative iliac BMB.
(a) The MIP of staging PET/CT shows extensive nodal disease involvement and multifocal marrow uptake affecting the axial and appendicular skeleton.
(b) Coronal fused PET/CT image shows the most avid marrow lesion in the right proximal femur (SUV_{BM} 5.0).
(c) The MIP of interim PET/CT 3 months later after R-CHOP chemotherapy shows complete resolution of the hypermetabolic lymphadenopathy and marrow foci.
(d) The corresponding coronal fused PET/CT image shows complete resolution of the right femoral uptake, concordant with the disease response elsewhere.
MIP: maximum intensity projection; PET/CT: fused positron emission tomography and computed tomography; BMB: bone marrow biopsy; SUV_{BM}: maximum standardized uptake value of focal uptake; R-CHOP: chemotherapy regime comprised of rituximab, cyclophosphamide, hydroxydaunorubicin, vincristine and prednisolone.

Table 1.

Indolent NHL	BMB +ve (*n*)	BMB -ve (*n*)	TP	TN	FP	FN	Total
PET/CT -ve							
Pattern: Normal	4	20	0	20	0	4	24
PET/CT +ve							
Pattern: Diffuse	14	1	14	0	1	0	15
Pattern: Focal	6	1	7	0	0	0	7

Fig.1.

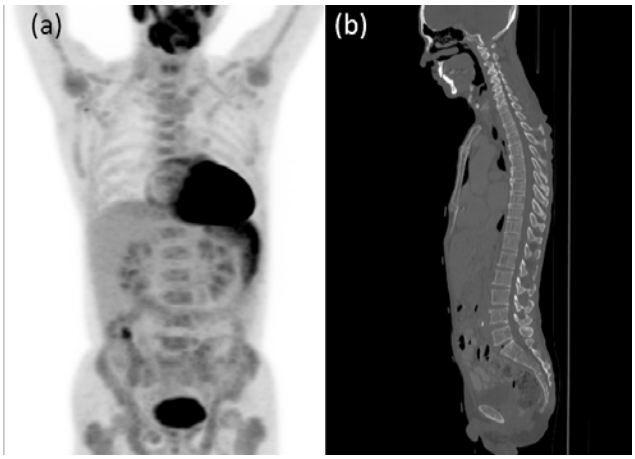

Fig.2.

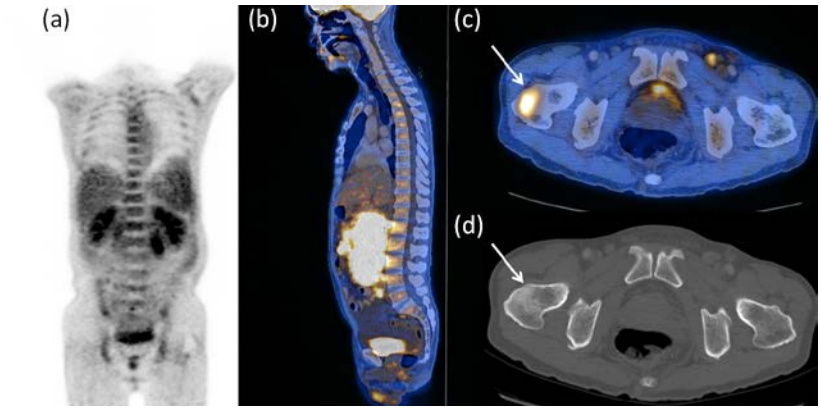

Fig.3.